1,3,4-Oxadiazole-Containing Polymers as Electron-Injection and Blue Electroluminescent Materials in Polymer Light-Emitting Diodes

Q. Pei* and Y. Yang

UNIAX Corporation, 6780 Cortona Drive, Santa Barbara, California 93117

Received March 20, 1995. Revised Manuscript Received May 26, 1995[⊗]

We report the synthesis, characterization, and optical properties of three 1,3,4-oxadiazole-containing polymers with different solubility and conjugation length (repeating units of phenylene and oxadiazole). Among them, the polymer with the shortest conjugation length (2 phenylene and one oxadiazole rings) has the widest $\pi-\pi^*$ bandgap and is not fluorescent. As an electron-injection material, it has been successfully used to improve the quantum efficiency of polymer light-emitting diodes (LEDs) using dialkoxy derivatives of poly(1,4-phenylenevinylene) as the electroluminescent layer and aluminum as the cathode. The second polymer, with an additional oxadiazole ring in the conjugated segment, is also an electron-injection polymer. This extra oxadiazole ring further enhances the electron transport property and has lowered the LED operating voltage more than the first polymer. The third 1,3,4-oxadiazole-containing polymer, with an even longer conjugation length, has strong blue fluorescence. Blue LEDs have been fabricated using this polymer as the electroluminescent layer, conducting polyaniline as the hole-injection layer, calcium as the cathode, and the first 1,3,4-oxadiazole-containing polymer as the electron-injection layer. These devices emitted a bright blue light, with 4.5 V of turn-on voltage and 0.1% of external quantum efficiency.

Introduction

Polymer light-emitting diodes (LEDs), based on conjugated polymers or polymers with conjugated segments or pendant groups, have recently attracted attention because of their potential use in display technology.[1-10] Typical polymer LEDs are composed of a thin polymer layer sandwiched between two metal electrodes. Under forward bias, electrons are injected from the cathode into the π^* orbital, while holes are injected from the anode into the π orbital of the polymer. The recombination of the injected electrons and holes in the polymer layer generates exitons which may radiatively decay. The characteristics of a polymer LED are determined by the tunneling of both holes and electrons through the interface barriers which is caused by the band offset between the electroluminescent polymer and the electrodes.[11,12] A significant difference in the barrier height at the polymer/cathode and polymer/anode interfaces results in unbalanced hole and electron injections, therefore dramatically reducing the photon/electron quantum efficiency of the devices. By selecting the proper anode and cathode materials, whose work-function respectively match the π and π^* orbitals of the electroluminescent polymer, one can significantly improve the balance of charge injections.[11-13] Alternatively, charge balance can also be achieved by selecting or synthesizing electroluminescent polymers whose π and π^* orbitals respectively match the work function of the anode and cathode materials.[14] Since candidates in these strategies are limited, materials with high charge-injection capability have been used to successfully improve the balance of hole and electron injections.[1d,2de,5b,15] These materials are blended in or used

[⊗] Abstract published in *Advance ACS Abstracts,* July 15, 1995.

(1) (a) Burroughes, J. H.; Bradley, D. D. C.; Brown, A. R.; Marks, R. N.; Mackay, K.; Friend, R. H.; Burns, P. L.; Holmes, A. B. *Nature* **1990**, *347*, 539. (b) Burn, P. L.; Holmes, A. B.; Kraft, A.; Bradley, D. D. C.; Brown, A. R.; Friend, R. H.; Gymer, R. W. *Nature* **1992**, *356*, 47. (c) Burn, P. L.; Holmes, A. B.; Kraft, A.; Bradley, D. D. C.; Brown, A. R.; Friend, R. H. *J. Chem. Soc., Chem. Commun.* **1992**, 32. (d) Brown, A. R.; Bradley, D. D. C.; Burn, P. L.; Burroughes, J. H.; Friend, R. H.; Greenham, N. C.; Holmes, A. B.; Kraft, A. *Appl Phys. Lett.* **1992**, *61*, 2793.

(2) (a) Braun, D.; Heeger, A. J. *Appl. Phys. Lett.* **1991**, *58*, 1982. (b) Braun, D.; Gustafsson, G.; McBranch, D.; Heeger, A. J. *J. Appl. Phys.* **1992**, *72*, 564. (c) Gustafsson, G.; Cao, Y.; Treacy, G. M.; Klavetter, F.; Colaneri, N.; Heeger, A. J. *Nature* **1992**, *357*, 477. Aratani, S. (d) Zhang, C.; Pakbaz, K.; Hoger, S.; Wudl, F.; Heeger, A. J. *J. Electron Mater.* **1993**, *22*, 745. (e) Zhang, C.; von Seggern, H.; Pakbaz, K.; Kraabel, B.; Schmidt, H. W.; Heeger, A. J. *Synth. Met.* **1994**, *62*, 35.

(3) (a) Grem, G.; Leditzky, G.; Ullrich, B.; Leising, G. *Adv. Mater* **1992**, *4*, 36. (b) Grem, G.; Leising, G. *Synth. Met.* **1993**, *55–57*, 4105.

(4) (a) Yang, Z.; Sokolik, I.; Karasz, F. E. *Macromolecules* **1993**, *26*, 1188. (b) Sokolik, I.; Yang, Z.; Karasz, F. E.; Morton, D. C. *J. Appl. Phys.* **1993**, *74*, 3584.

(5) (a) Ohmori, Y.; Uchida, M.; Muro, K.; Yoshino, K. *Jpn. J. Appl. Phys.* **1991**, *30*, L1941. (b) Ohmori, Y.; Uchida, M.; Muro, K.; Yoshino, K. *Solid State Commun.* **1991**, *80*, 605. (c) Ohmori, Y.; Morishima, C.; Uchida, M.; Yoshino, K. *Jpn. J. Appl. Phys.* **1992**, *31*, L568.

(6) Vestweber, H.; Greiner, U. A.; Lemmer.; Mahrt, R. F.; Richert, Heitz, W.; Bassler, H. *Adv. Mater.* **1992**, *4*, 661.

(7) Gmeiner, J.; Karg, S.; Meier, M.; Riess, W.; Strohriegl, P.; Schwoerer, M. *Acta Polym.* **1993**, *44*, 201.

(8) Gao, Y.; Park, K. T.; Hsieh, B. R. *J. Appl. Phys.* **1993**, *73*, 7894.

(9) (a) Berggren, M.; Gustafsson, G.; Inganas, O.; Andersson, M. R.; Wennerstrom, O.; Hjertberg, T. *Adv. Mater.* **1994**, *6*, 488. (b) Berggren, M.; Inganas, O.; Gustafsson, G.; Rasmusson, J.; Andersson, M. R.; Hjertberg, T.; Wennerstrom, O. *Nature* **1994**, *372*, 444.

(10) Malliaras, G. G.; Herrema, J. K.; Wildeman, J.; Wieringa, R. H.; Gill, R. E.; Lampoura, S. S.; Hadziioannou, G. *Adv. Mater.* **1993**, *5*, 721.

(11) (a) Bradley, D. D. C. *Synth. Met.* **1993**, *54*, 401. (b) Marks, R. N.; Bradley, D. F. D. C.; Jackson, R. W.; Burn, P. L.; Holmes, A. B. *Synth. Met.* **1993**, *55–57*, 4128.

(12) Parker, I. D. *J. Appl. Phys.* **1994**, *75*, 1656.

(13) Doi, S.; Kuwabara, M.; Noguchi, T.; Ohnishi, T. *Synth. Met.* **1993**, *55–57*, 4174.

(14) Greenham, N. C.; Moratti, S. C.; Bradley, D. D. C.; Friend, R. H.; Holmes, A. B. *Nature* **1993**, *365*, 628.

0897-4756/95/2807-1568$09.00/0

as an additional layer to, the electroluminescent polymer layer. A hole-injection material will facilitate a hole injection from the anode, while an electron-injection material will facilitate an electron injection from the cathode.[16] In fact, charge-injection (or charge-transporting) layers have been widely used in small organic molecule LEDs.[17]

While a number of hole-injection polymers are available and have been used in polymer LEDs with success, there are few known polymers with good electron-injection capability.[14,18] Several small organic molecules, such as 2-(4-biphenylyl)-5-(4-*tert*-butylphenyl)-1,3,4-oxadiazole (PBD), have been successfully used as electron-injection material to improve the balance of charge injections and to increase the photon/electron quantum efficiency.[1d,2e,15a,19] The improved performance is believed to result from the high electron affinity of the oxadiazole ring in the molecules.[20] Recently, several analogues of PBD have been synthesized and tested to be good electron-injection material.[21] Therefore, it is expected that the polymeric analogues of PBD, i.e., oxadiazole-containing polymers, are also a good electron-injection material. In addition, the use of polymers has the following advantages: (1) polymers are easily processed into thin films by spin-casting, and (2) crystallization occurs much slower in polymer films than in films of small organic molecules. It has been noted that thin films of PBD in LEDs crystallized over time which caused device failure, especially when devices were operated at temperatures above 70 °C.[22]

Oxadiazole-containing polymers have been investigated since the 1960s as a thermally stable material.[20b,23-25] Most of them are, however, infusible and insoluble in common organic solvents. Certain efforts have been made to prepare processable and thermally stable oxadiazole-containing polymers. Only a few have been used in electronic devices. There are a few reports on using an oxadiazole-containing polymer, poly(1,4-phenylene-1,3,4-oxadiazole), as a charge-transporting material. Though its conductivity can be upgraded to semiconducting and metallic levels by either doping or pyrolysis,[26] this polymer has long been known to be an electrically insulating material and has been used as the insulating layer in metal–insulator–semiconductor diodes.[27] It has also been used as a charge transfer layer in electrophotographic devices.[28]

In this paper, we present the synthesis of two 1,3,4-oxadiazole-containing polymers **I**[29] and **II**, and their application in polymer LEDs, as the electron-injection

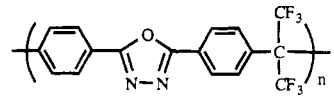

(I)

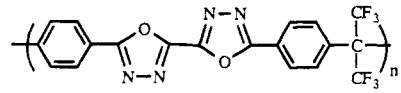

(II)

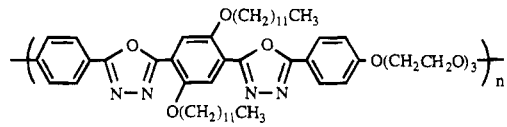

(III)

material. We found that, with short conjugation length, **I** and **II** have a wide π–π^* energy gap. They are not fluorescent, but they can be used as an electron-injection layer to significantly improve the photon/electron quantum efficiency of LEDs using soluble derivatives of poly(1,4-phenylenevinylene) as the electroluminescent material.

On the other hand, the oxadiazole-containing small molecules also form an important class of organic scintillators and laser dyes with high photoluminescent efficiency.[30,31] A lot of efforts have been made to synthesize new types of molecules with varied fluorescence color and solubility.[31] One wide use of these oxadiazole-containing molecules has been as optical brightening agents in synthetic polymeric materials.

(15) (a) Hosokawa, C.; Kawasaki, N.; Sakamoto, S.; Kusumoto, T. *Appl. Phys. Lett.* **1992**, *61*, 2503. b) Uchida, M.; Ohmori, Y.; Noguchi, T.; Ohnishi, T.; Yoshino, K. *Jpn. J. Appl. Phys.* **1993**, *32*, L921.

(16) Parker, I. D.; Pei, Q.; Marrocco, M. *Appl. Phys. Lett.* **1994**, *65*, 1272.

(17) (a) Tang, C. W.; Van Slyke, S. A. *Appl. Phys. Lett.* **1987**, *51*, 913. (b) Tang, C. W.; Van Slyke, S. A. *J. Appl. Phys.* **1989**, *65*, 3610. (c) Adachi, C.; Tokito, S.; Tsutsui, T.; Saito, S. *Jpn. J. Appl. Phys.* **1988**, *27*, 59. (d) Adachi, C.; Tsutsui, T.; Saito, S. *Appl. Phys. Lett.* **1989**, *55*, 1489.

(18) (a) Turner, S. R.; AuClair, C. *Macromolecules* **1976**, *9*, 868. (b) Tazuke, S.; Nagahara, H. *J. Polym. Sci., Polym. Lett. Ed.* **1978**, *16*, 525. (c) Shirota, Y. In *Functional Monomers and Polymers*; Takemoto, K., Inaki, Y., Ottenbrite, R. M., Eds.; 1989; p 283.

(19) Aratani, S.; Zhang, C.; Pakbaz, K.; Hoger, S.; Wudl, F.; Heeger, A. J. *J. Electron. Mater.* **1994**, *23*, 453.

(20) (a) Johnson, R. N.; Farnham, A. G.; Clendinning, R. A.; Hale, W. F. *J. Polym. Sci., Polym. Chem. Ed.* **1977**, *18*, 354. (b) Hedrick, J. L.; Twieg, R. *Macromolecules* **1992**, *25*, 2021.

(21) (a) Hamada, Y.; Adachi, C.; Tsutsui, T.; Saito, S. *Nippon Kagaku Kaishi* **1991**, 1540. (b) Tsutsui, T.; Aminaka, E.; Fujita, Y.; Hamada, Y.; Saito, S. *Synth. Met.* **1993**, *57*, 4157.

(22) (a) Adachi, C.; Tsutsui, T.; Saito, S. *Appl. Phys. Lett.* **1990**, *56*, 799. (b) Adachi, C.; Tsutsui, T.; Saito, S. *Appl. Phys. Lett.* **1990**, *57*, 531.

(23) (a) Hasegawa, M. *Encycl. Polym. Sci. Eng.* **1969**, *11*, 169–187. (b) Cassidy, P. E.; Fawcett, N. C. *J. Macromol. Sci.–Rev. Macromol. Chem.* **1979**, *C17*, 209. (c) Nanjian, M. J. *Encycl. Polym. Sci. Eng.* **1985**, *12*, 322–339.

(24) (a) Frazer, A. F.; Sweeny, W.; Wallenberger, F. T. *J. Polym. Sci. Part A* **1964**, *2*, 1157. (b) Kovacs, H. N.; Delman, A. D. *J. Polym. Sci. Part A-1* **1970**, *8*, 869. (c) Iwakura, Y.; Uno, K.; Hara, S. *J. Polym. Sci. Part A* **1965**, *3*, 45. (d) Preston, J.; Black, W. B. *J. Polym. Sci. Polym. Lett.* **1966**, *4*, 267. (e) Yakubovich, A. Y.; Gitina, R. M.; Zaitseva, E. L.; Markova, G. S.; Simonov, A. P. *Vysokomol. Soedin., Ser. A* **1971**, *12*, 2520. (f) Kovacs, H. N.; Delman, A. D.; Simms, B. B. U.S. Patent 3,567,698, 1971. (g) Korshak, V. V.; Vinogradova, S. V.; Vygodskii, Y. S. *J. Macromol. Sci.–Rev. Macromol. Chem.* **1974**, *C11*, 45. (h) Sato, M.; Yokoyama, M. *J. Polym. Sci., Polym. Chem. Ed.* **1980**, *18*, 2751.

(25) (a) Brydon, D. L.; Fisher, I. S.; Emans, J. E.; Smith, D. M.; MacDonald, W. A. *Polymer* **1989**, *30*, 619. (b) Mansour, E. M. E.; Kandil, S. H.; Hassan, H. H. A. M.; Shaban, M. A. E. *Eur. Polym. J.* **1990**, *26*, 951. (c) Connell, J. W.; Hergenrother, P. M.; Wolf, P. *Polymer*, **1992**, *33*, 3507. (d) Sinigersky, V.; Wegner, G.; Schopov, I. *Eur. Polym. J.* **1993**, *29*, 617. (e) Fitch, J. W.; Cassidy, P. E.; Weikel, W. J.; Lewis, T. M.; Trial, T.; Burgess, L.; March, J. L.; Glowe, D. E.; Rolls, G. C. *Polymer* **1993**, *34*, 4796.

(26) (a) Murakami, M.; Yasujima, H.; Yumoto, Y.; Mizogami, S.; Yoshimura, S. *Solid State Commun.* **1983**, *45*, 1085. (b) Shinozuka, S.; Tomizuka, Y.; Nojiri, A. Japanese Patent JP 60,44,550, **1985**. (c) Tsutsui, T.; Fukuta, Y.; Hara, T.; Saito, S. *Polym. J.* **1987**, *19*, 719.

(27) Tsunoda, S.; Koezuka, H.; Kurata, T.; Yanaura, S.; Ando, T. *J. Polym. Sci., Polym. Phys.* **1988**, *26*, 1697.

(28) (a) Manilio, M.; Franko, K. French Patent 1,493,172, 1967. (b) Morimoto, K. Japan Patent JP 43,26,709, 1967. (c) Kakuta, A.; Mori, Y.; Takano, S.; Sawada, M.; Shibuya, I. *J. Imaging Technol.* **1985**, *11*, 7.

(29) (a) Livshits, B. R.; Vinogradova, S. V.; Knunyunts, I. L.; Berestneva, G. L.; Dymoshits, T. K. L. *Vysokomol. Soyed. Ser. A* **1973**, *15*, 961. (b) Hensema, E. R.; Sena, M. E. R.; Mulder, M. H. V.; Smolders, C. A. *J. Polym. Sci. Part A: Polym. Chem.* **1994**, *32*, 527.

(30) (a) Birks, J. B. *Photophysics of aromatic molecules*; Interscience: London, 1970; p 134. (b) Maeda, M. *Laser Dyes*; Academic Press: Tokyo, 1984; p 262. (c) Jiaxing, P.; Yadong, L.; Zhenheng, G. *Chem. J. Chinese Univ. (Engl. Ed.)* **1985**, *1*, 82.

(31) (a) Hayes, F. N.; Rogers, B. S.; Ott, D. G. *J. Am. Chem. Soc.* **1955**, *77*, 1850. (b) Ciba Limited, British Patent 746,047, 1956. (c) Rangnekar, D. W.; Phadke, R. C. *Dyes Pigm.* **1985**, *6*, 293. (d) Hironaka, Y.; Tokailin, H.; Hosokawa, C.; Kusumoto, T. *PCT Int. Appl.* **1993**, WO 93,01,252.

Some 1,3,4-oxadiazole-containing polymers, such as poly(1,4-phenylene-1,3,4-oxadiazole), also fluoresces under UV irradiation.[32] In light of the current interest in polymer LEDs, in particular blue LEDs,[33-35] it is interesting to prepare soluble oxadiazole-containing polymers that are useful as a new type of blue electroluminescent materials.

In this paper, we also present the synthesis of a 1,3,4-oxadiazole-containing polymer **III**. With a longer conjugation length than both **I** and **II**, **III** has a narrower $\pi-\pi^*$ energy gap and is intensively fluorescent with a blue emission. Bright blue electroluminescence from **III** has been observed. Blue polymer LEDs reported in the literature have mainly used poly(1,4-phenylene)s,[3,33] derivatives of poly(1,4-phenylenevinylene),[2e,4a,15a,34] poly(alkylfluorene)s,[5a] poly(thiophene)s,[9b,10] and others.[16,35]

Experimental Section

1. General Information. Chemicals received from commercial sources were ACS reagent grade and were used without further purification. All manipulations were performed in air under ambient conditions, unless otherwise stated. Gas chromatography to check purity of compounds was performed on a Hewlett-Packard 5280 GC with a Hewlett-Packard 5971 mass-selective detector. Melting point was observed under a microscope and was not corrected. Infrared spectra were taken of KBr pellets or dip-cast films using a Midac FT-IR split beam spectrophotometer. Elemental analysis was performed by Galbraith Laboratories. Solution NMR spectra were recorded on a Varian 500 MHz in $CDCl_3$ with TMS standard. UV-vis absorption spectra were recorded on an HP 8452A diode array UV-vis spectrophotometer. Photoluminescent and electroluminescent spectra were recorded using an Oriel Multispec CCD array spectrometer. Absolute values for the photoluminescent quantum efficiency were calculated by using an integrating sphere to measure the total power of the emitted light from the samples.

2. Materials. *Polymer I:* Phosphorous pentoxide (3.0 g) was dissolved in methanesulfonic acid (30 g). Into this solution, hydrazine monohydrochloride (0.40 g, 5.8 mmol) and 4,4′-(hexafluoroisopropylidene)bis(benzoic acid) (1.9 g, 5.0 mmol) were added while stirring. The suspension was stirred at 100 °C for 4 h and subsequently at 140 °C for 3.5 h. After cooling, the viscous solution was poured slowly into water while stirring to precipitate white fibers. The fibers were washed with water and air-dried before being dissolved in tetrahydrofuran and reprecipitated into methanol. Polymer **I** of a quantitative yield was collected by filtration and subsequently dried in vacuum at 100 °C. η_{inh} = 0.52 dl/g (0.2 g/dL solution in tetrahydrofuran, 25 °C). Elemental analysis found: C, 54.9; H, 2.4; F, 28.7; N, 7.4. Calculated for $C_{17}H_8F_6N_2O$: C, 55.1; H, 2.2; F, 30.8; N, 7.6.

Poly(hydrazide) IV: 4,4′-(Hexafluoroisopropylidene)bis(benzoic acid) was reacted with excess thionyl chloride for 17 h. Excess thionyl chloride was removed in vacuum to leave quantitative amount of 4,4′-(hexafluoroisopropylidene)bis(benzoyl chloride). Into 0.275 g (2.33 mmol) of oxalic dihydrazide in 15 mL of *N,N*-dimethylacetamide containing 0.75 g of LiCl, 1.0 g (2.33 mmol) of 4,4′-(hexafluoroisopropylidene)bis(benzoyl chloride) was added at 0 °C. After 30 min of stirring, the reaction mixture was neutralized with lithium carbonate and then poured into water to coagulate the product. Poly(hydrazide) (0.81 g, 74%) was collected after being dried in vacuum at 80 °C. η_{inh} = 0.62 dL/g (0.18% solution in *N,N*-dimethylacetamide, 25 °C).

Polymer II: Poly(hydrazide) **IV** (0.633 g) was gently refluxed in excess phosphorous oxychloride for 4 h. After cooling, the reaction solution was slowly poured into cold water while stirring to effect coagulation of a grayish solid which weighed 0.50 g (80%) after being washed with water and dried in vacuum at 80 °C. η_{inh} = 0.35 dL/g (0.2% solution in *N,N*-dimethylformamide, 25 °C). Elemental analysis found: C, 51.8; H, 2.0; F, 24.9; N, 12.4. Calculated for $C_{19}H_8F_6N_4O_2$: C, 52.1; H, 1.8; F, 26.0; N, 12.8.

1,2-Bis[2-(4-(chloroformyl)phenoxy)ethoxy]ethane (V): Ethyl 4-hydroxybenzoate (27.74 g, 0.167 mol), 1,2-bis(chloroethoxy)-ethane (15.61 g, 0.0835 mol), and sodium carbonate (17.70 g, 0.167 mol) in 35 mL of *N,N*-dimethylformamide were refluxed for 24 h. The reaction mixture was cooled and poured into ice water. The precipitate was collected by filtration and washed with water. The off-white solid was refluxed for 2 h with 25 g of NaOH dissolved in 250 mL of ethanol. After being cooled, the milky reaction mixture was poured into 400 mL of water to render a clear solution. Concentrated HCl was then added to rendor a final solution pH ~1-2. The white precipitate was collected by filtration and washed with water. After recrystallization from *N,N*-dimethylformamide/ethanol and subsequent drying in vacuum at 80 °C, 19.4 g of 1,2-bis[2-(4-chloroformylphenoxy)ethoxy]ethane was yielded; mp 228-231 °C (lit.[36] 227-229.5 °C). The diacid was refluxed in excess thionyl chloride for 2 h when a clear solution had been effected. Excess thionyl chloride was removed by distillation with forced nitrogen flow. The residue solidified after being cooled. It was washed with dry hexanes and dried in vacuum to yield 21.01 g (70% overall) of the diacyl chloride; mp 68 °C (lit.[36] 66-67 °C).

2,5-Didodecyloxyterephthalic dihydrazide (VI): Diethyl 2,5-dihydroxyterephthalate (38.1 g, 0.15 mol), 1-bromododecane (149.5 g, 0.60 mol), and potassium carbonate (82.9 g, 0.60 mol) were refluxed for 80 h in 300 mL of acetone. The mixture was then cooled and filtered. The solid was washed repeatedly with acetone. After solvent of the combined filtrate was stripped off, the residue was dissolved in ether, washed with 5% KOH aqueous solution, and dried with magnesium sulfate. The solvent was stripped off. The residue was recrystallized twice from ethanol to yield 56.70 g of white crystals of diethyl 2,5-didodecyloxyterephthalate; mp 56-60 °C (lit.[37] 57 °C). It was reacted with excess hydrazine monohydrate in 200 mL of methanol. The mixture was filtered. The solid was recrystallized from ethanol, and dried in a vacuum at 80 °C to yield 39.2 g (47% overall) of white crystals; mp 105-107 °C.

Polyhydrazide VII: **V** (1.0 g, 2.34 mmol) was added, while stirring, into a solution containing 1.32 g (2.34 mmol) of **VI** and 1.97 g (4.8 mmol) of triethylamine in 30 mL of chloroform. After 10 min of vigorous stirring, the solution was poured into methanol. The precipitate was collected by filtration, washed with methanol and water, and then dried in a vacuum at 80 °C to yield 2.1 g (93%) of white product. ^{1}H NMR ($CDCl_3$) δ = 0.77-0.82 (s, 6H); 1.10-1.34 (s, low-field shoulders, 32 H); 1.38-1.45 (br, 4H); 1.88-1.95 (br, 4H); 3.65-3.70 (s, 4H); 3.77-3.82 (broad, 4H); 3.94-4.05 (broad, 8 H); 6.71-6.82 (br, 6 H); 7.43-7.63 (br, 4H); 7.65-7.75 (br, 4 H). η_{inh} = 0.30 dL/g (0.2% solution in chloroform, 25 °C).

Polymer III: The polyhydrazide **VII** (1.0 g) was gently refluxed in 10 mL of $POCl_3$ for 5 h. The clear solution was poured into ice water. The yellow precipitate was collected by filtration and washed with water and acetone. Further purification was carried out by dissoluting twice into chloro-

(32) Poly(1,4-phenylene-1,3,4-oxadiazole) fluoresces blue light both in the solid state and in solutions in concentrated sulforic acid.

(33) (a) Huber, J.; Mullen, K.; Schenk, H.; Scherf, U.; Stehlin, T.; Stern, R. *Acta Polym.* **1994**, *45*, 244. (b) Yamamoto, T.; Inoue, T.; Kanbara, T. *Jpn. J. Appl. Phys.* **1994**, *33*, L250. (c) Jing, W. X.; Kraft, A.; Moratti, S. C.; Gruner, J.; Cacialli, F.; Hamer, P. J.; Holmes, A. B.; Friend, R. H. *Synth. Met.* **1994**, *67*, 161. (d) Gruner, J.; Hamer, P. J.; Friend, R. H.; Huber, H. J.; Scherf, U.; Holmes, A. B. *Adv. Mater.* **1994**, *6*, 748.

(34) (a) von Seggern, H.; Schmidt-Winkel, P.; Zhang, C.; Schmidt, H. W. *Macromol. Chem. Phys.* **1994**, *195*, 2023.

(35) (a) Kido, J.; Hongawa, K.; Okuyama, K.; Nagai, K. *Appl. Phys. Lett.* **1993**, *63*, 2627. (b) Lachinov, A. N.; Zolotukhin, M. G.; Antipin, V. A.; Valeeva, I. L. *Angew. Makromol. Chem.* **1994**, *214*, 11. (c) Osaheni, J. A.; Jenekhe, S. A. *Macromolecules* **1994**, *27*, 739. (d) Patridge, R. H. UK Patent No. 74 44 704, 1974. (e) Hu, B.; Yang, Z.; Karasz, F. E. *J. Appl. Phys.* **1994**, *76*, 2419.

(36) Volken, W.; Yoon, D. Y. *Macromolecules* **1989**, *22*, 3849.

(37) Ballauff, M. *Makromol. Chem. Rapid Commun.* **1986**, *7*, 407.

form and precipitating in acetone. After drying in a vacuum at 80 °C, 0.85 g of yellow powders were yielded. ^{1}H NMR ($CDCl_3$) δ 0.85–0.89 (s, 6H); 1.24–1.36 (s, low-field shoulders, 32 H); 1.42–1.58 (br, 4H); 1.75–1.92 (br, 4H); 3.77–3.79 (s, 4H); 3.85–4.20 (br, 12 H); 6.79–8.05 (multipeaks, 10 H). η_{inh} = 0.25 dL/g (0.2% solution in chloroform, 25 °C). Elemental analysis found: C, 70.3; H, 8.2; N, 6.1. Calculated for $C_{13}H_{18}NO_2$: C, 70.9; H, 8.2; N, 6.4.

Poly[5-(2'-ethylhexyloxy)-2-methoxy-1,4-phenylenevinylene] (MEH-PPV) and poly[2,5-bis(cholestanoxy)-1,4-phenylene vinylene] (BCHA-PPV): Both were prepared according to the methods developed by Wudl et al.[38]

3. Device Fabrication. Two types of polymer light-emitting diodes were fabricated for this research: (1) LEDs for the study of **I** and **II** as electron injection materials; (2) blue LEDs using **III** as the electroluminescent material. All the polymer LEDs fabricated in this research were multilayer devices. Indium–tin oxide (ITO) coated glass (200 Ω per square) was used as the substrate. For the study of electron injection materials, MEH-PPV and BCHA-PPV were used as the electroluminescent polymers. MEH-PPV and BCHA-PPV layers (typically 1300 Å thick) were spun-cast from solutions in xylene onto ITO. A layer of **I** or **II** was deposited on top of the electroluminescent layer by spin-casting from solutions in 2-butanone or *N,N*-dimethylformamide. Finally, a metal cathode (Al) was deposited on top of the polymer layers by evaporation at pressures around 5×10^{-7} Torr and evaporation rates of 1–5 Å/s. For the study of blue LEDs, a layer of **III** (1000 Å) was spin-cast from solution in chloroform onto ITO. A layer of **I** was then deposited on top of **III** by spin-casting from solutions in 2-butanone or *N,N*-dimethylformamide. Finally, a metal cathode (Ca) was deposited at the same condition as above. To lower the operating voltage of the blue LEDs, a thin layer of PANI-DBSA (conducting polyaniline doped with dodecylbenzenesulfonic acid) was used between the ITO and the electroluminescent layer in some devices.[44] This layer was prepared by spin-casting the PANI-DBSA solution in toluene[39] onto ITO before spin-casting polymer **III**. Diode areas were 12 mm^2. All fabrication and testing steps were performed under an inert gas atmosphere. In forward bias, the ITO electrode was wired as the anode.

Results and Discussion

1. Polymer Synthesis. Incorporation of the polar and branched 4,4'-(hexafluoroisopropylidene) moiety into a polymer backbone has been shown to be an effective way to substantially increase the solubility of the polymer.[40] The 4,4'-(hexafluoroisopropylidene) moiety has also been incorporated into the backbone of 1,3,4-oxadiazole-containing polymers.[29,41] Polymer **I** had been prepared by cyclodehydration of the corresponding poly(hydrazide) at high temperatures.[29] The polyhydrazide was, in turn, prepared by a low-temperature polycondensation of the dihydrazide and dichloride of 4,4'-(hexafluoroisopropylidene)bis(benzoic acid). **I** had also been prepared by a one-port polycondensation and cyclodehydration reaction in polyphosphoric acid, using 4,4'-(hexafluoroisopropylidene)bis(benzoic acid) and hydrazine as monomers.[29b] We have prepared **I** also by a one-port reaction, but used methanesulfonic acid containing 10 wt % phosphorous pentoxide dissolved therein as the polymerization reagent.[25e,42] The reaction might proceed through polyhydrazide intermediate which was further cyclodehydrated to form the 1,3,4-oxadiazole rings. High polymers were obtained at a high temperature and with a long reaction time. At 140 °C, the viscosity of the polymerization solution increased with time, and the solution became a stirrable slurry after a few hours.

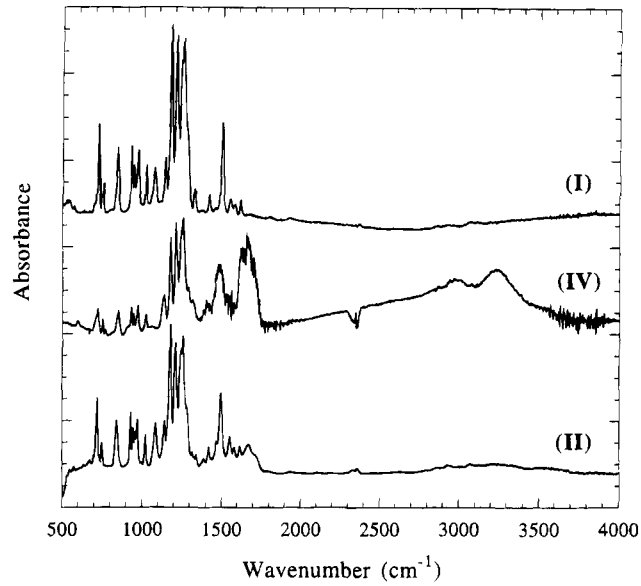

Figure 1. FTIR spectra of thin films of polymers **I**, **II**, and **IV**.

Polymer **I**, prepared by our method, had a higher viscosity than those prepared by the previous methods, indicating a higher molecular weight. The elemental analysis result agreed with its chemical structure. The infrared spectrum of **I** displayed in Figure 1 shows three strong absorption peaks at 1170–1270 cm^{-1} due to C–F stretching, and a peak at 1500 cm^{-1} due to the 1,3,4-oxadiazole ring stretching.[23b] The absence of absorption peaks in the range 1640–1700 cm^{-1} (C=O stretching) and in the range 3200–3400 cm^{-1} (N–H stretching) indicates completion of the cyclodehydration reaction.

The solubility test showed that **I** is readily soluble in many organic solvents including tetrahydrofuran, pyridine, *N,N*-dimethylformamide, *N,N*-dimethylacetamide, chlorinated hydrocarbons, and methyl ethyl ketone. It is insoluble in alcohols and low-polarity solvents such as hexanes, toluene, and xylenes. Homogeneous, colorless, and tough films of **I** can be cast from solutions.

Polymer **II** has also been prepared by the one-port method, using 4,4'-(hexafluoroisopropylidene)bis(benzoic acid) and oxalic dihydrazide as monomers, and methanesulfonic acid containing 10 wt % phosphorous pentoxide dissolved therein as the polymerization reagent. The product was a brown polymer of low molecular weight. Inherent viscosity in *N,N*-dimethylformamide at 25 °C was 0.15 dL/g, therefore, we turned to the two-step synthesis via poly(hydrazide). Polycondensation of 4,4'-(hexafluoroisopropylidene)bis(benzoyl chloride) with an equimolar amount of oxalic dihydrazide in *N,N*-dimethylacetamide at 0 °C yielded the poly(hydrazide)

(38) (a) Wudl, F.; Allemand, P. M.; Srdanov, G.; Ni, Z.; McBranch, D. In *Materials for Nonlinear Optics: Chemical Perspectives*; Marder, S. R., Sohn, J. E., Stucky, G. D., Eds.; American Chemical Society: Washington, DC, 1991; pp 683–686. (b) Wudl, F.; Hoger, S.; Zhang, C.; Pakbaz, K.; Heeger, A. J. *Polym. Prepr.* **1993**, *34*, 197.

(39) Cao, Y.; Smith, P.; Heeger, A. J. *Synth. Met.* **1992**, *48*, 91.

(40) Harris, F. W.; Lanier, L. H. In *Structure-Solubility Relationships in Polymers*; Harris, F. W., Seymour, R. B., Eds.; Academic Press: London, 1977.

(41) Fitch, J. W.; Cassidy, P. E.; Weikel, W. J.; Lewis, T. M.; Trial, T.; Burgess, L.; March, J. L.; Glowe, D. E.; Rolls, G. C. *Polymer* **1993**, *34*, 4796.

(42) Ueda, M.; Sato, M.; Mochizuki, A. *Macromolecules* **1985**, *18*, 2723.

Scheme 1

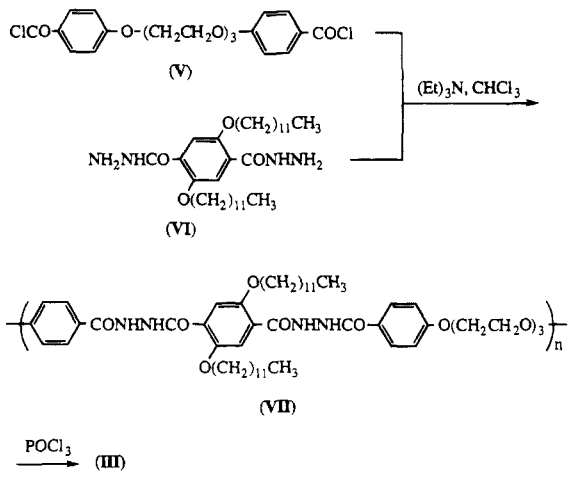

IV of the following structure:

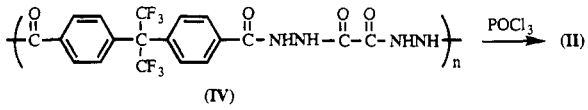

Its infrared spectrum displayed in Figure 1 shows the characteristic peaks at 1170−1270 cm^{-1} due to C−F stretching, a broad peak around 1650 cm^{-1} due to C=O stretching, and a broad peak at 3250 cm^{-1} due to N−H stretching. The poly(hydrazide) **IV** was converted to oxadiazole-containing polymer **II** by gently refluxing it in excess phosphorous oxychloride. Polymer **II** collected after purification was a light yellow solid. Its inherent viscosity in *N,N*-dimethylformamide at 25 °C was 0.35 dL/g. An elemental analysis result of **II** agreed with its chemical structure. The infrared spectrum of **II**, also displayed in Figure 1, shows three strong absorption peaks at 1170−1270 cm^{-1} due to C−F stretching, and a peak at 1500 cm^{-1} due to 1,3,4-oxadiazole ring stretching. The weak peak at 1650 cm^{-1} and the negligible absorption in the range 3200−3400 cm^{-1} probably indicate that the end groups of the polymer chain are mainly carboxyl.

Polymer **II** is less soluble than **I**, due to the increased length of the rigid segments. However, **II** is still readily soluble in *N,N*-dimethylformamide, *N,N*-dimethylacetamide, and tetrahydrofuran. Homogeneous, colorless, and tough films of **II** can be cast from solutions.

Polymer **III** has been synthesized in several steps, as displayed in Scheme 1.

The synthesis of monomer **V** started with the preparation of a diester from ethyl 4-hydroxybenzoate and 1,2-bis(chloroethoxy)ethane by typical Williamson ether synthesis condition. The diester was hydrolyzed and subsequently acidified to afford a diacid, which was reacted with thionyl chloride to lead to the diacyl chloride **V**. The overall yield was 70%. The synthesis of monomer **VI** started with the preparation of a diester from diethyl 2,5-dihydroxyterephthalate and 1-bromododecane. The diester was reacted with hydrazine to afford the dihydrazide **VI**. The overall yield was 47%. Polycondensation of monomers **V** and **VI** in chloroform at room temperature afforded the polyhydrazide **VII**. The chemical structure of **VII** was confirmed by ^1H NMR. Its infrared spectrum displayed in Figure 2 shows the characteristic peaks at 1625, 3160, and 3350 cm^{-1} due to the dihydrazide groups.

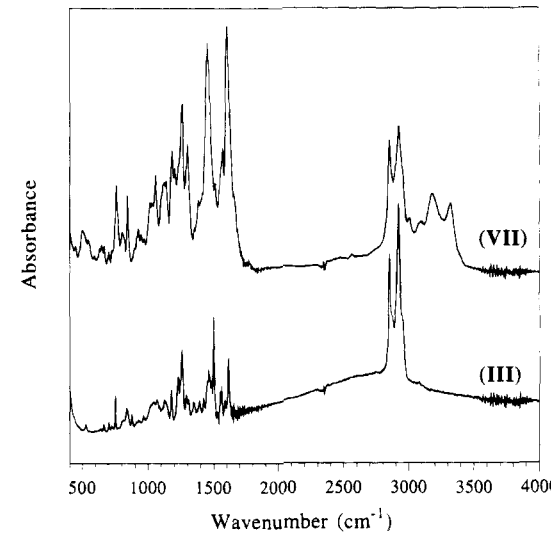

Figure 2. FTIR spectra of polymers **III** and **VII** (in KBr pellets).

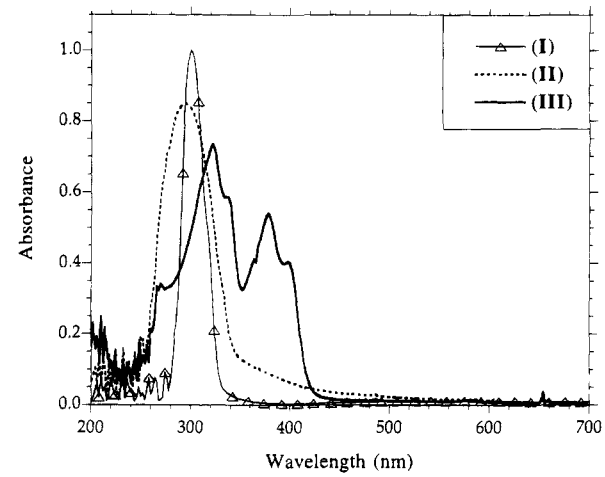

Figure 3. UV−vis absorption spectra of thin films of polymers **I**−**III**.

VII was converted to the oxadiazole-containing polymer **III** by gentle reflux in phosphorous oxychloride. The chemical structure of **III** was confirmed by its ^1H NMR spectrum and elemental analysis result. The infrared spectrum of **III** is also displayed in Figure 2. The characteristic peaks due to dihydrazide groups has disappeared, indicative of effective cyclodehydration. Instead, a new peak at 1490 cm^{-1} appears due to 1,3,4-oxadiazole rings. The weak peak at 1620 cm^{-1}, in the spectrum of **III**, may be attributable to carboxylic end groups of the polymer chain.

2. Optical Absorption and Photoluminescence. The UV−vis absorption spectra of the three oxadiazole-containing polymers **I**−**III** are displayed in Figure 3. The absorption peak red shifts and the half-peak width of the peak increases from polymer **I** to **II** to **III** in the same trend with the increasing length of the conjugated segment in these polymers. Polymer **III** has two absorption peaks, each with a few shoulders. The absorption extends into the visible range, and the material is light yellow. Polymers **I** and **II** have little absorption in the visible range. They are colorless. The bandgaps between the highest occupied molecular or-

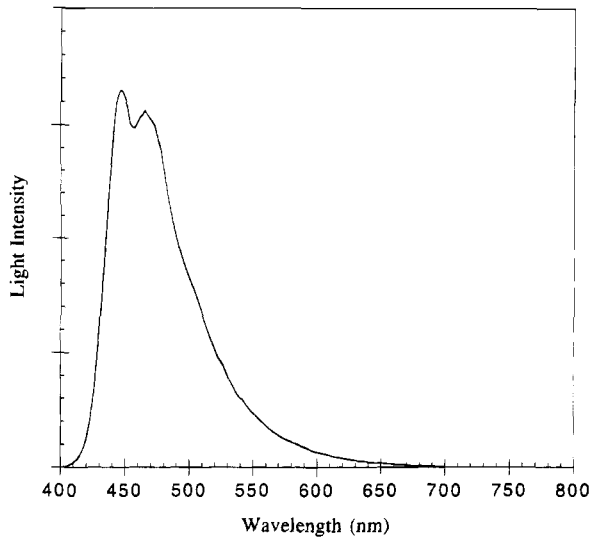

Figure 4. Photoluminescent spectrum of a thin film of **III**.

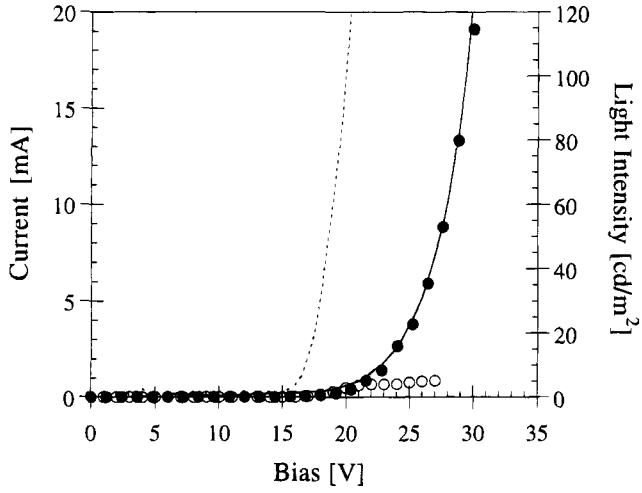

Figure 5. Current vs bias (lines) and light vs bias (circles) characteristics for ITO/MEH-PPV/Al (dashed line, open circles) and ITO/MEH-PPV/**I**/Al (solid line, filled circles) devices. The layer of **I** is 270 Å thick.

bital (π) and the lowest unoccupied molecular orbital (π^*), taken from the onset of the absorption spectra, are 3.8, 3.5, and 2.9 eV, for **I**–**III**, respectively. The wide bandgaps of **I** and **II** are desirable for use as a charge-injection material, especially in blue light-emitting diodes (LEDs), because radiative electron–hole recombination is consequently confined to the emissive layer of narrower bandgap.

Under ultraviolet light irradiation, polymers **I** and **II** did not emit visible light, whereas **III** was strongly fluorescent with blue emission. Figure 4 displays the photoluminescent spectrum of **III** with 366 nm UV irradiation. Two peaks at 445 and 465 nm are observed. The quantum efficiency of the spin-cast thin films were measured to be 35 ± 3%. The emission spectrum overlaps very little with the absorption spectrum, therefore, reabsorption of the emitted light by the material itself is negligible. Both the negligible self-absorption and the high photoluminescent quantum efficiency indicate that polymer **III** may be explored as an ideal blue electroluminescent material.

3. Polymers I and II as Electron-Injection Materials in LEDs. Figure 5 displays the current-light-bias curves of polymer LEDs, using MEH-PPV as the electroluminescent polymer and Al as the cathode, with and without a layer of polymer **I** between the MEH-PPV layer and the Al cathode. Without a **I** layer, the current turned on at a lower voltage, but the device never emitted a bright light. In comparison, the orange light, emitted from the device with a layer of **I**, was observable even under normal room illumination. The light-bias curve followed the same pattern as the current-bias curve, indicative of balanced electron and hole injections. By using the layer of **I**, the external quantum efficiency (electron/photon) of the device increased by a factor of at least 50 from 0.001–0.002% in devices without **I** to about 0.1% in devices having the layer of **I**.

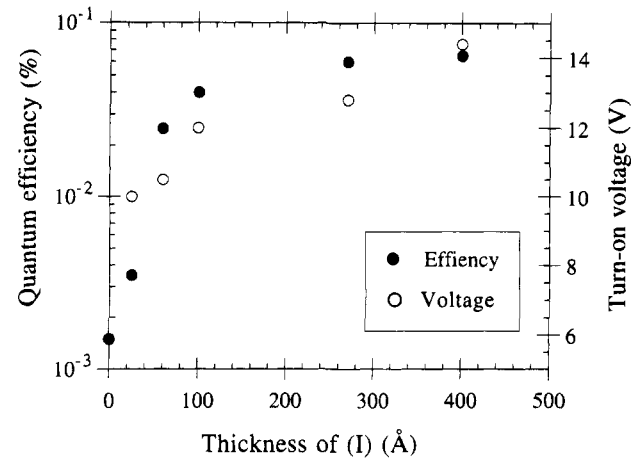

Figure 6. Quantum efficiency and turn-on voltage of ITO/MEH-PPV/**I**/Al devices as a function of the thickness of **I** layer.

Table 1. Quantum Efficiency of Polymer LEDs with and without a Layer of I

electroluminescent layer	quantum efficiency			
	MEH-PPV		BCHA-PPV	
cathode	Ca	Al	Ca	Al
without **I**	0.36%	0.002%	0.37%	0.03%
with **I**	0.26%	0.08%	0.30%	0.30%

Figure 6 shows the quantum efficiency as a function of the thickness of the **I** layer. The efficiency first increases with thickness but soon saturates. The turn-on voltage, defined as the voltage bias at which the light output is read as 1 mV detected by the silicon photodiode placed above the polymer LEDs (a light output level which is just observable to the naked eye in the dark), also increases as the layer of **I** becomes thicker. The turn-on voltage of the device without a layer of **I** is not shown in the figure, because the light intensity increases very slowly with voltage bias without a sharp turn-on.

The quantum efficiencies of several devices are listed in Table 1 for comparison. For devices using MEH-PPV as the electroluminescent layer, the layer **I** has only small effect on the efficiency when the cathode is Ca. However, significant improvement is seen when the cathode is Al. Similar effects are observed in devices using poly(2,5-bischolestanoxy-1,4-phenylenevinylene) (BCHA-PPV) as the electroluminescent layer. We found that the efficiency of the Al cathode devices is close to that of the Ca cathode devices when a layer of **I** is present; while without this layer, the efficiencies differ by more than 2 orders of magnitude.

The disadvantage of Ca as a cathode is obvious; Ca is not stable in air, thus requiring that devices be hermetically sealed. In addition, reaction might occur at the interface with the active luminescent polymer.[43] The high quantum efficiency and brightness of the devices, using polymer **I** layer and Al cathode, should be promising for practical applications of the polymer LEDs. These devices remained operative after 1 year of storage in air, without encapsulation.

Electroluminescent results, obtained from MEH-PPV and BCHA-PPV devices without a layer of polymer **I**, have been published earlier.[2] The electroluminescent medium in the devices with a layer of **I** continues to be the PPV layer (MEH-PPV or BCHA-PPV) rather than **I**. The bright orange color of the light, emitted from the MEH-PPV device with an Al cathode and a layer of **I**, has the same spectrum as that of the electroluminescence from a simple ITO/MEH-PPV/Ca device; both are the same as the photoluminescent spectrum of MEH-PPV. The brilliant yellow color of the light emitted from the BCHA-PPV device is also the same as the photoluminescence color of BCHA-PPV.

We suggest that the layer of polymer **I** acts as an electron-injection medium in these devices. Since the π^* orbital of MEH-PPV is much higher (by 1.5 eV) than the work function of Al,[12] electron injection from Al into MEH-PPV is severely inhibited by the barrier at the interface, while holes can be readily injected from the anode (ITO) into MEH-PPV. This imbalance in charge injection results in low quantum efficiency in an ITO/MEH-PPV/Al device (most of the holes pass through the electroluminescent layer before encountering electrons). Such devices are effectively one-carrier (hole only) devices as indicated by the differences in the current-bias and light-bias curves of the device shown in Figure 5.

The oxadiazole-containing **I** is expected to be a better electron-accepting polymer than MEH-PPV, due to the presence of the 1,3,4-oxadiazole rings. The barrier for electron injection from the cathode into **I** at the **I**/Al interface is, therefore, lower than that at the MEH-PPV/Al interface. The electrons injected into **I** transport through **I** into MEH-PPV by a mechanism which remains unclear. The imbalance of hole and electron injection into MEH-PPV is, therefore, alleviated, and the device efficiency is increased. The improved balance of opposite sign charge injection is reflected in Figure 5 where the current-bias and light-bias curves are nearly identical. The small difference in quantum efficiency of the ITO/BCHA-PPV/**I**/Ca and ITO/BCHA-PPV/**I**/Al devices, as well as the approximately 1 order of magnitude difference in efficiency observed in corresponding ITO/BCHA-PPV/Ca and ITO/BCHA-PPV/Al devices, as shown in Table 1, results from the same mechanism operative in the MEH-PPV devices.

In addition to its role as an electron-injection medium, the layer of **I** might also act as a hole barrier to block the transport of holes from the electroluminescent medium into the metal electrode.[16]

Since electron injection has been facilitated, one would have expected that the devices with **I** would turn on at lower voltage in contrast to what has been observed in this study. Moreover, Figure 6 shows that the turn-on voltage increases with the thickness of the layer of **I**. To understand this, we suggest that although polymer **I** is a good electron acceptor, it is a relatively poor electron-transporting material; i.e., the transport through **I** is mobility-limited. The layer of **I** presents a high series resistance to electrons injected at the interface to transport through **I** into MEH-PPV. This series resistance increases with the thickness of the layer. Therefore, there are mixed effects on the turn-on voltage resulting from the layer of **I**: the improved electron injection tends to decrease the turn-on voltage, while the formation of a high resistance transport layer tends to increase the turn-on voltage.

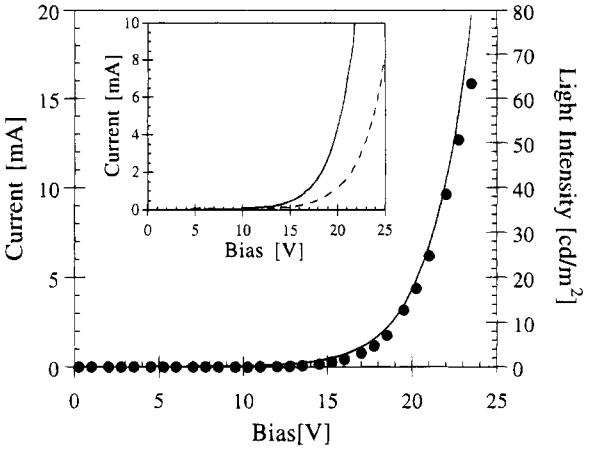

Figure 7. Current vs bias (line) and light vs bias (filled circles) characteristics for an ITO/MEH-PPV/**II**/Al device. The layer of **II** is 300 Å thick. Inset: the current vs bias curves of ITO/MEH-PPV/**I**/Al (dashed line) and ITO/MEH-PPV/**II**/Al (solid line) devices.

This analysis is supported by the optical absorption spectrum of polymer **I** displayed in Figure 3. Both the wide π–π^* bandgap (3.8 eV) and the narrow absorption band are characteristics of restricted π-electron conjugation. Charge transport in the material is limited by hopping of charges between the conjugated segments. On the other hand, MEH-PPV is a typical conjugated polymer with a long π-electron conjugation length. It has a narrow bandgap and a wide absorption band. Polymer **I** is much more resistant (low mobility) to electron transport than MEH-PPV is. By this analysis, polymer **II** is expected to be a better electron-transporting material than **I**, because **II** has a narrower bandgap (3.5 eV) and much wider absorption band as shown in Figure 3.

Devices using polymer **II** instead of **I** as the electron injection layer were fabricated and the current-light-bias curves of the ITO/MEH-PPV/**II**/Al device are displayed in Figure 7. The current-bias and light-bias curves follow a similar pattern, indicative of balanced electron and hole injections. As the inset of Figure 7 shows, the turn-on voltage of the ITO/MEH-PPV/**II**/Al device is considerably lower than that of the ITO/MEH-PPV/**I**/Al device, probably because polymer **II** is a better electron-transporting material than polymer **I**.

The external quantum efficiency of the ITO/MEH-PPV/**II**/Al devices was about 0.1%, comparable to that of the ITO/MEH-PPV/**I**/Al devices. Devices using **II** as the electron-injection layer and silver or indium as the cathode were also fabricated. The turn-on voltage and

(43) Gao, Y.; Park, K. T.; Hsieh, B. R. *J. Appl. Phys.* **1993**, *73*, 7894.
(44) (a) Yang, Y.; Heeger, A. J. *Appl. Phys. Lett.* **1994**, *64*, 1245. (b) Yang, Y.; Westerweele, E.; Zhang, C.; Smith, P.; Heeger, A. J. *J. Appl. Phys. Lett.* **1995**, *77*, 694.

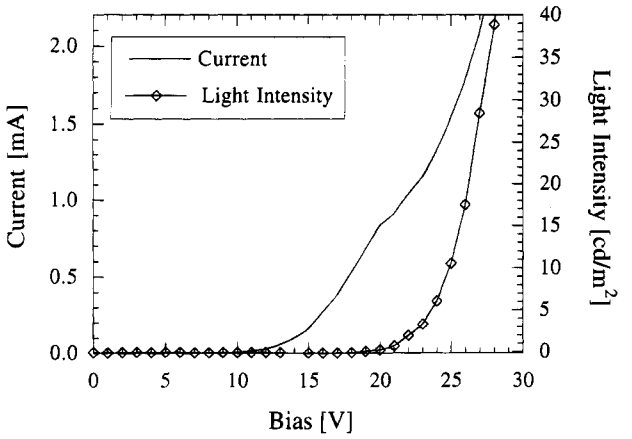

Figure 8. Current vs bias and light vs bias characteristics of an ITO/**III**/**I**/Ca device.

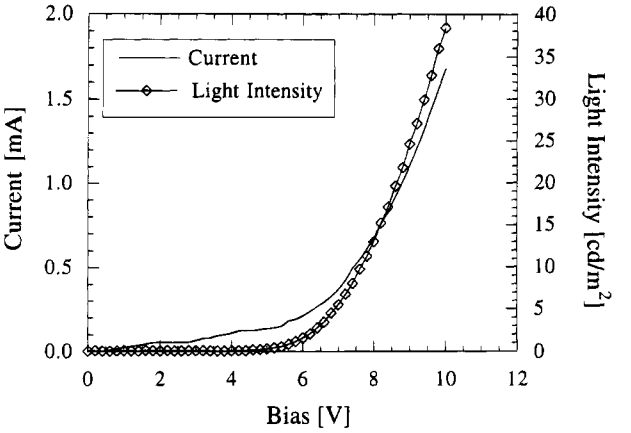

Figure 9. Current vs bias and light vs bias characteristics of an ITO/PANI-DBSA/**III**/**I**/Ca device.

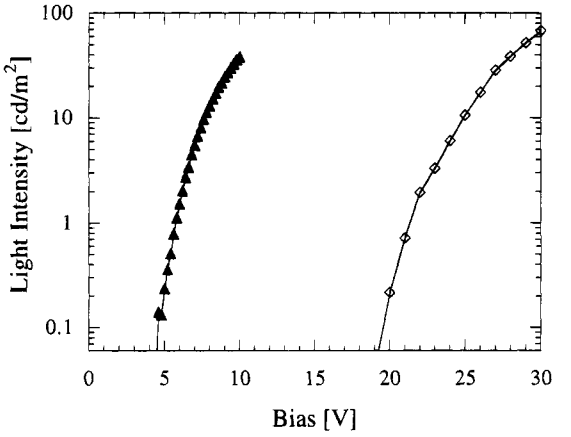

Figure 10. Comparison of the turn-on voltages of ITO/**III**/**I**/Ca and ITO/PANI-DBSA/**III**/**I**/Ca devices.

quantum efficiency of these devices were close to those of the devices using aluminum as the cathode. Polymer **II** is an attractive electron-injection material for the fabrication of air-stable light-emitting diodes.

4. Polymer III as Blue Electroluminescent Material. LEDs using ITO as the anode, calcium as the cathode, and polymer **III** as the electroluminescent layer, ITO/**III**/Ca, did not emit light at bias voltages up to 100 V. After an additional layer of **I** had been used, the device, ITO/**III**/**I**/Ca, emitted light at high voltages. Figure 8 shows the typical current-light-bias curves of these devices. Though the current (or charge injection) turns on at 11 V, it is not until 20 V that the light turns on, an indication of imbalance in the injection of opposite charges. The external quantum efficiency of this device was around 0.025%.

The emitted light was sky blue with an EL spectrum almost identical to the photoluminescent spectrum of **III**. Since **I** is not fluorescent, the electroluminescent material in this device was **III**.

To increase the quantum efficiency and lower the turn-on voltage of the blue LEDs, an additional layer of conducting polyaniline was used between the ITO and **III** to enhance hole injection into the electroluminescent **III** layer.[44] Figure 9 shows the typical current-light-bias curves of an ITO/PANI-DBSA/**III**/**I**/Ca device. Although there is a small leakage current at low voltages, the current and voltage both turn on at approximately 4–6 V, indicative of a better balance in the injection of opposite charges. ITO/PANI-DBSA/**III**/**I**/Ca devices have been fabricated with external quantum efficiencies up to 0.1%. The intensity of the emitted blue light was 40 cd/m^2 at a drive voltage of 10 V.

Figure 10 clearly shows the importance of the PANI-DBSA layer as both a hole-injection and transport material. The turn-on voltages of the ITO/**III**/**I**/Ca and ITO/PANI-DBSA/**III**/**I**/Ca devices, are 19 and 4.5 V, respectively. The dramatically reduced turn-on voltage is due to the higher work-function of PANI-DBSA compared to that of ITO[44] and improved contact between PANI/**III** interface. Hole-injection into **III** from the ITO/PANI-DBSA composite electrode is improved to the point of being comparable to the electron-injection at the cathode. At the same time, the high hole mobility in conducting PANI-DBSA is also helpful in significantly reducing the turn-on voltage.

Conclusion

Oxadiazole-containing polymers **I**–**III**, with different solubility and conjugation length, have been synthesized. Among them, **I** has the widest π–π^* bandgap and is not fluorescent. As an electron-injection material, it has been successfully used to improve the quantum efficiency of LEDs using dialkoxy derivatives of PPV as the electroluminescent layer and aluminum as the cathode. **II** has an additional oxadiazole ring in the conjugated segment and is also an electron-injection polymer. This extra oxadiazole ring further enhances the electron-transport property and has lowered the LED operating voltage more than **I** has done. **III** has an even longer conjugation length, and has an efficient blue fluorescence. LEDs, using **III** as the electroluminescent layer, emitted a bright blue light, with 4.5 V of turn-on voltage and 0.1% of external quantum efficiency.

CM950133X